

Treating late-onset Tay Sachs disease: Brain delivery with a dual trojan horse protein

Esther Osher,^{1,2,11} Yossi Anis,^{1,11} Ruth Singer-Shapiro,¹ Nataly Urshanski,¹ Tamar Unger,³ Shira Albeck,³ Oren Bogin,¹ Gary Weisinger,^{1,12} Fortune Kohen,⁴ Avi Valevski,⁵ Aviva Fattal-Valevski,⁶ Liora Sagi,⁶ Michal Weitman,⁷ Yulia Shenberger,⁷ Nadav Sagiv,¹ Ruth Navon,⁸ Meir Wilchek,⁹ and Naftali Stern^{1,2,10}

¹The Sagol Center for Epigenetics and Institute of Endocrinology, Metabolism and Hypertension, Tel Aviv-Sourasky Medical Center, Tel Aviv, Israel; ²Faculty of Medicine, Tel Aviv University, Tel Aviv, Israel; ³Department of Structural Proteomics, Weizmann Institute of Science, Rehovot, Israel; ⁴Department of Immunology and Regenerative Biology, Weizmann Institute of Science, Rehovot, Israel; ⁵Geha Mental Health Center, Petach-Tikva, Israel; ⁶Pediatric Neurology Unit, Tel Aviv-Sourasky Medical Center, Tel Aviv, Israel; ⁷The Chemistry Department, Bar Ilan University, Ramat Gan, Israel; ⁸Department of Human Molecular Genetics & Biochemistry, Faculty of Medicine, Tel Aviv University, Tel Aviv, Israel; ⁹Department of Biomolecular Sciences, Weizmann Institute of Science, Rehovot, Israel; ¹⁰The Sagol School of Neuroscience, Tel Aviv University, Tel Aviv, Israel

Tay-Sachs (TS) disease is a neurodegenerative disease resulting from mutations in the gene encoding the α -subunit (HEXA) of lysosomal β -hexosaminidase A (HexA). We report that (1) recombinant HEXA alone increased HexA activity and decreased GM2 content in human TS glial cells and peripheral mononuclear blood cells; 2) a recombinant chimeric protein composed of HEXA linked to two blood-brain barrier (BBB) entry elements, a transferrin receptor binding sequence and granulocyte-colony stimulating factor, associates with HEXB *in vitro*; reaches human cultured TS cells lysosomes and mouse brain cells, especially neurons, *in vivo*; lowers GM2 in cultured human TS cells; lowers whole brain GM2 concentration by approximately 40% within 6 weeks, when injected intravenously (IV) to adult TS-mutant mice mimicking the slow course of late-onset TS; and increases forelimbs grip strength. Hence, a chimeric protein equipped with dual BBB entry elements can transport a large protein such as HEXA to the brain, decrease the accumulation of GM2, and improve muscle strength, thereby providing potential treatment for late-onset TS.

INTRODUCTION

Tay-Sachs (TS) disease is an autosomal recessive neurodegenerative disease resulting from deficiency of lysosomal β -hexosaminidase A (HexA) activity due to inherited mutations in the α -subunit gene. As a result, the enzyme is inactive, which leads to the accumulation of the GM2 ganglioside in neuronal lysosomes and to extra-lysosomal GM2 aggregates. This eventually results in severe cellular dysfunction, cell death, and progressive neurodegeneration.¹⁻³

In human and other mammalian tissues, β -hexosaminidase exists in two major forms: HexA, a heterodimer of the α - and β -subunits ($\alpha\beta$) encoded by two different genes, HEXA and HEXB, and a homodimeric HexB ($\beta\beta$).¹ A third form, HexS, consisting of the homodimer $\alpha\alpha$, normally comprises only a minor fraction of β -hexosaminidase, but is more prominently expressed in Sandhoff disease, which results from inherited defects in the HEXB gene.

The formation of the HexA is controlled by complex mechanisms culminating in the association of the α - and β -subunits. Both subunits undergo a succession of post-translational modifications in the endoplasmic reticulum (ER), which include removal of the signal peptide on the amino terminal end, N-glycosylation with high-mannose oligosaccharides,⁴ followed by formation of disulfide bonds and tertiary folding of the polypeptides. There is controversy regarding whether $\alpha\beta$ assembly occurs in the ER or the Golgi apparatus, but either the enzyme or the polypeptides are transported to the Golgi apparatus such that the α/β ratio seems to be well-regulated.⁵

Mannose-6-phosphate (M6P) recognition elements are generated in the Golgi apparatus, as the mannose residues of the glycosylated amino acids α asparagine115, α asparagine 295, and β asparagine 84 are preferentially phosphorylated.⁴ This modification enables the M6P receptor in the Golgi apparatus to recognize and target the enzyme to the lysosomes.⁶ In the lysosome, the enzyme is subjected to final processing, including the maturation of the α -chain, which includes removal of the precursor peptide (i.e., the polypeptide sequence leucine 23-leucine 90⁷). Consequently, HexA can degrade GM2 in the presence of the GM2 activator protein.

Late-onset TS (LOTS), a rare disorder, first described in 1973,⁸ is a slow variant of the more widely recognized infantile TS disease. Owing to less severe enzymatic deficiency, its clinical onset is delayed to late childhood through early adulthood, with a slower deterioration

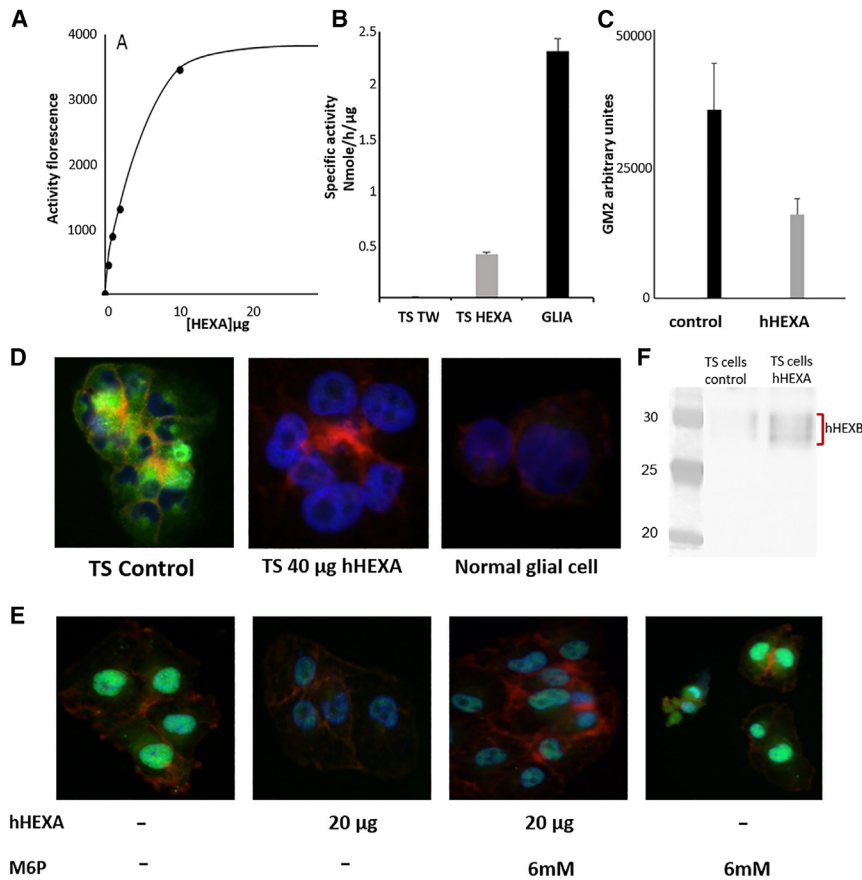
Received 26 April 2024; accepted 13 July 2024;
<https://doi.org/10.1016/j.omtm.2024.101300>.

¹¹These authors contributed equally

¹²Deceased

Correspondence: Naftali Stern, MD, The Sagol Center for Epigenetics, Institute of Endocrinology, Metabolism and Hypertension, Tel Aviv Sourasky Medical Center and Faculty of Medicine, Tel Aviv University, 6 Weizmann Street, Tel Aviv, Israel.
E-mail: nafstern66@gmail.com





compared with the rapidly progressive, lethal infantile form. Its estimated incidence in the Ashkenazi Jewish population of 1 in 135,000; the incidence in the non-Jewish population is unknown, but may approximate that of infantile TS or Sandhoff disease (1 in 300,000) in this group.⁹ A detailed literature review on LOTS has been recently published.¹⁰ No effective treatment is currently available for TS or LOTS disease. Enzyme replacement therapy (ERT) is a strategy that has been clinically approved for some lysosomal storage diseases such as Gaucher disease.¹¹ However, even though normal HexA can now be prepared, ERT has thus far not been offered to TS patients since the enzyme cannot cross the blood-brain barrier (BBB).¹²

To overcome this problem and enable transport of replacement protein for TS, we reasoned that a functional protein smaller than the entire approximately 1,000-Kd HexA might be easier to transport across the BBB. We also assumed that protein composed of the replacement enzyme sequence linked to two independent entry elements, each independently capable of passage through the BBB might allow its effective transport through the BBB. That partial correction of HexA activity in TS *in vitro* by selective replacement of the α chain in HexA-deficient fibroblasts was suggested by one study,¹³ but not confirmed in another report.¹⁴ Here, we re-tested this approach in

a human TS cell line *in vitro*. We then applied it *in vivo* in a TS mouse model by engineering a chimeric protein in which the alpha subunit was fused, via a flexible peptide linker, to two BBB entry elements known to each independently cross the BBB: the granulocyte-colony stimulating factor (G-CSF) followed by a small transferrin receptor binding sequence.^{15–19}

RESULTS

Synthesis and activity of HEXA and HEXB

Human HEXA (hHEXA) and murine HEXA (mHEXA) were produced as described in [materials and methods](#) (under production of HEXA), for the chimeric protein (see below; [Figure S1](#)).

We then examined the enzymatic activity of the recombinant purified HEXA alone and in cultured TS cells. [Figure 1A](#) shows the dose-related effect of recombinant hHEXA (0–30 $\mu\text{g}/\text{mL}$ [0–0.34 nmol/L; 24 h) on HexA activity in the presence of the substrate 4-methylumbelliferyl- β -N-acetylglucosamine-6-sulfate (MUGS). [Figure 1B](#) depicts the effect of HEXA added to cultured TS glial cells. While significant cell HexA activity was clearly achieved in the presence of hHEXA (80 $\mu\text{g}/\text{mL}$ [0.9 nmol/L] over 24 h), cellular activity amounted to approximately 20% of that seen in normal cultured glial cells. hHEXA added to TS cells also decreased cell GM2 by approximately 55%, as measured by liquid chromatography-tandem mass spectrometry (LC-MS/MS) ([Figure 1C](#)) or nearly completely as depicted by immuno-fluorescent staining ([Figure 1D](#)). [Figures 1E](#) and [1F](#) show TS

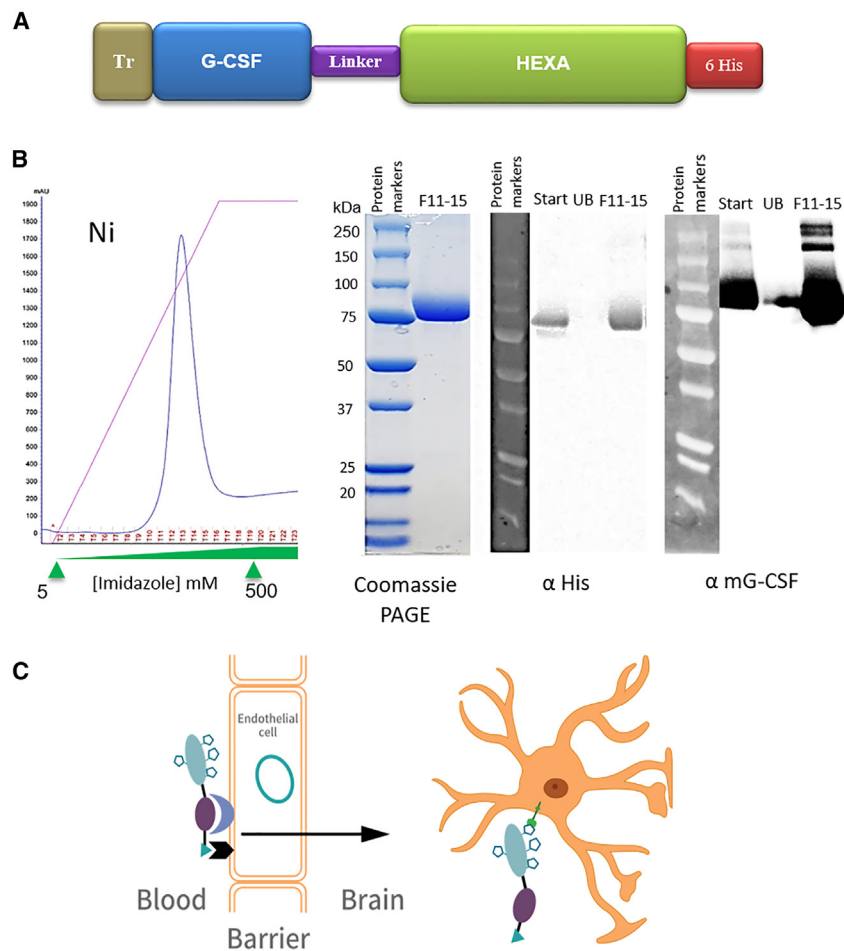


Figure 2. HEXA recombinant proteins (HEXA alone, or as a fusion protein with G-CSF or Tr-G-CSF) were produced in XP293 cells and then purified using the same procedure

Shown is an example of mTr-G-CSF-HEXA, whose schematic structure is presented in (A). Proteins were purified in one-step on a Ni column. The protein was detected by Coomassie SDS-PAGE and western blots using anti-tetra-His (C-terminus) and anti-mouse-G-CSF (N-terminus) (B). The putative entry mechanism of mTr-G-CSF-HEXA is summarized in (C). Two separate ligands, Tr-binding peptide and G-CSF, independently capable of binding to two distinct BBB-expressed receptors, Tr receptor and G-CSF receptors, are included in the fusion protein and are linked to HEXA through a flexible linker. The new engineered protein thus crosses the BBB and then reaches further, into GM2-accumulating cells within the brain.

ceptor binding ligand,¹⁹ murine G-CSF, a flexible linker, the full mHEXA and a poly-6 histidine repeat (His tag) at the carboxyterminal (His tag). This chimeric protein is referred to as mouse-Transferrin-G-CSF-HEXA (mTr-G-CSF-HEXA). Figure 2B depicts the purification (left) of Tr-G-CSF-HEXA on an imidazole gradient, showing the elution peak, followed by Coomassie blue blot staining and western blots (with anti-tetra-His antibody or anti-mouse-G-CSF antibody) of the purified fusion protein (middle and right, respectively).

In solution, the synthesized mTr-G-CSF-HEXA is found in an oligomeric state that is buffer formula dependent, as determined by size exclusion analysis (Figure S2A). In all solution formulas we found only a minor portion as aggregate (>400 kDa). The protein in formulas A and C is mostly at the tetrameric state (approximately 400 kDa). In the solution formula B, both the trimeric (approximately 300 kDa) and dimeric state (approximately 200 kDa) were dominant. The results are presented in Figure S6.

mTr-G-CASF-HEXA associates with mHEXB and vice versa *in vitro* (Figure S2B). Further, the association of mTr-G-CSF-HEXA with mHEXB is dose dependent and parallels a dose-related increase in measured enzymatic activity. (Figure S2C).

In the Tr-G-CSF-HEXA protein, both HEXA and G-CSF retained their distinct respective activities, as shown in Figure 3. Since G-CSF's effect on cell proliferation requires its binding to membrane receptors for G-CSF, it follows that, despite its compounded structure, mTr-G-CSF-HEXA is able to bind to the cell surface, where G-CSF serves as an agonist (Figure 3A) on its receptor while still allowing HEXA to express its enzymatic function *in vitro* (Figure 3B) and within the cell, after cell penetration (see next). This was likely possible owing to the

glial cells, incubated in with hHEXA in the presence or absence of M6P. In short-term (≤ 3 h) incubations, M6P inhibited the ability of added external HEXA to effectively incorporated into TS cells. In longer incubations, M6P inhibited the ability of added HEXA to decrease GM2 in TS cells. This is consistent with the notion that externally added hHEXA penetrates the cells and may be then targeted intracellularly via the M6P receptor. We also prepared cell lysates from TS cells, which were first incubated with HEXA, followed by repeated washes. Cell lysates were first immuno-precipitated with anti-His antibody, and then probed with anti-HEXB antibody, as shown in Figure 1G, thus showing an HEXA/HEXB complex was present in HEXA-treated TS cells (see materials and methods). Finally, hHEXA increased HexA activity (MUGS) measured in peripheral blood mononuclear cells (PBMCs) isolated from four LOTS patients incubated without and with HEXA for 24 h and 48 h and lowered GM2 in these cells in culture (Figure S2). The clinical details of these LOTS patients are summarized in Table S1.

Engineered chimeric HexA proteins and their activity

We synthesized a fusion protein composed, in sequence, of five functional elements, as illustrated in Figure 2A: a short transferrin-re-

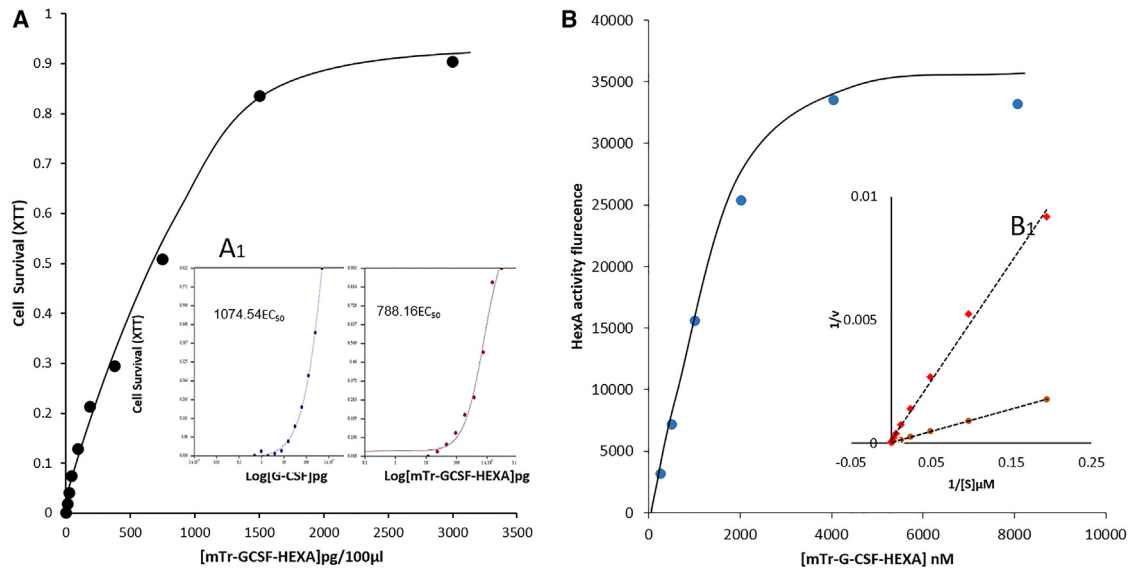


Figure 3. mTr-G-CSF-HEXA retains both HEXA enzymatic activity and G-CSF-related bioactivity

(A) Cell survival/ Effect of mTr-G-CSF-HEXA on cell survival is shown in black circles. Comparison between mTr-G-CSF-HEXA (red circles) and hG-CSF (Neupogen; blue circles) is depicted A1, where the proteins equally promote M-NFS-60 cell survival/proliferation. The experimental half maximal effective concentrations (EC_{50}) were 1074.54 pg/mL for Tr-G-CSF-HEXA and 788.16 pg/mL for hG-CSF. (B) HexA activity. Dose-dependent HexA enzymatic activity of mTr-G-CSF-HEXA alone is shown in A (blue circles). A1 depicts the comparison between mTr-G-CSF-HEXA (brown circles) and mHEXA (red squares). The apparent K_m was 225 μ M and 481 μ M, respectively.

proper separation by the two proteins afforded by the sufficiently long and flexible linker constructed for this chimeric protein.

We next incubated human TS glial cells with 80 μ g/mL (0.9 μ mol/L) mTr-G-CSF-HEXA or mG-CSF-HEXA for 18 h. After four washes, intracellular HexA enzymatic activity was measured by an assay in which the MUGS served as a substrate for HexA (see [materials and methods](#)). As shown in [Figure 4](#), the recombinant protein mTr-G-CSF-HEXA was able to enter cultured human TS glial cells ([Figure 4A](#)). The internalized protein was probed with anti-tetra-His antibody (seen in bright green), and partly colocalized with Lamp 2 (red fluorescence), a lysosomal protein, as shown by the merged bright yellow spots. mTr-G-CSF-HEXA and mG-CSF-HEXA also increased intracellular HexA activity ([Figure 4B](#)). [Figure 4C](#) depicts the colocalization of the internalized mTr-G-CSF-HEXA (again probed with anti-His antibody) with the intracellular HEXB probed with anti-HEXB antibodies. Further, hTr-G-CSF-HEXA ([Figure S4](#)) was able to lower human TS cell GM2.

mTr-G-CSF-HEXA decreases GM2 in the brain of TS mice

To examine whether or not IV injected mTr-G-CSF-HEXA could enter the brain, we tested for the presence of the protein in the brain *in vivo*. This was compared with the ability of peripherally administered (IV) equimolar dose of HEXA alone to gain excess to the brain. Using high magnitude confocal microscopy with immuno-fluorescent-detection ($\times 100$), mTr-G-CSF-HEXA, but not HEXA, was clearly present in the brain ([Figure 5A](#)) collected 3 h after its injection. The bright red staining represents the injected protein probed with a

rabbit anti-6-His tag antibody. Nuclei are visualized in blue (stained with DAPI). The preferential cytoplasmic localization of the injected protein can be more clearly seen in cells where mTr-G-CSF-HEXA, in red, is seen around the Dapi-stained nuclei. Specifically, mTr-G-CSF-HEXA was present in the cortex, thalamus, cerebellum, and hippocampus, and to a lesser degree at the septum ([Figure 5B](#)). Subsequent experiments showed that mTr-G-CSF-HEXA protein was still abundantly present in the brain of WT mice 3 days after injection and some could still be found even 7 days after IV administration of 1,000 μ g mG-CSF-HEXA ([Figure S5](#)).

We next examined the brain cell type into which the peripherally injected Tr-G-CSF was incorporated using antibodies to two markers, neuronal nuclear protein (NeuN), a nuclear protein specific for neuronal cells and glial fibrillary acidic protein (GFAP), a member of the cytoskeletal protein family expressed in glial cells. As shown in [Figure 6](#), Tr-G-CSF-HEXA was mostly incorporated into neuronal cells, but some uptake by glial cells was also detected.

In addition to the brain, mTr-G-CSF-HEXA could be seen in heart sections, renal cortical sections, and the spleen. There was no significant mTr-G-CSF-HEXA presence in the liver, possibly due to repaired degradation in liver cells, but this was not further explored ([Figure S2B](#)). Interestingly, despite the preservation of G-CSF activity within the Tr-G-CAS-HEXA fusion protein in the acute setting *in vitro*, after 6 weeks of bi-weekly IV injections of this protein, no changes in blood count could be noted between Tr-G-CSF-HEXA- and placebo-treated mice ([Table S2](#)).

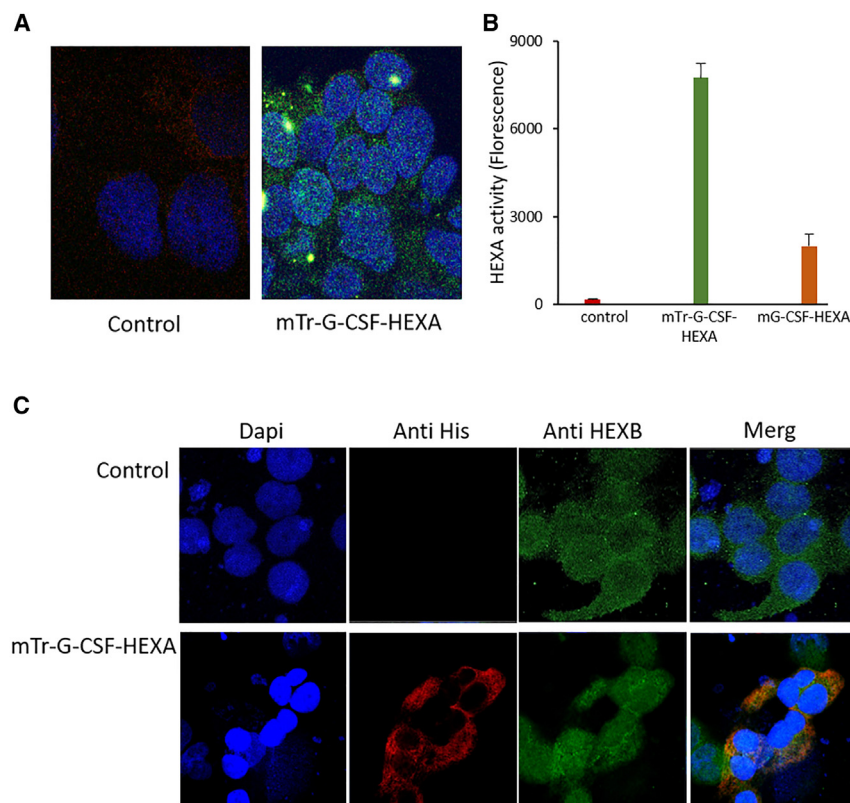


Figure 4. mTr-G-CSF-HEXA penetrate TS Glial cells and increase their HexA enzymatic activity

(A) Immuno-fluorescent staining of TS cells after initial incubation with 80 $\mu\text{g}/\text{mL}$ (0.9 μM) mTr-G-CSF-HEXA over 16h. The cellular uptake of mTr-G-CSF-HEXA is visualized using an anti-tetra-his antibody (in green) and the lysosomal distribution was tested with anti Lamp2 (in red, A). As a result, cellular HexA activity, assessed with MUGS, markedly increased ($p \leq 1.9 \times 10^{-5}$). (B). (C) Intracellular colocalization of mTr-G-CSF internalized by cultured TS cells (identified by anti-His antibodies in red) and endogenous HEXB, detected anti hHEXB (in green). The blue color represents nuclei stained with DAPI.

mTr-G-CSF-HEXA decreases GM2 in the brain of TS mice

Figure 7 depicts the effect of mTr-G-CSF-HEXA on brain GM2 concentration after chronic treatment in TS $\text{HEXA}^{-/-}$ mice. Twelve-month-old male TS $\text{HEXA}^{-/-}$ mice received IV injections (tail vein) of vehicle ($n = 49$) or 250 μg mTr-G-CSF-HEXA ($n = 55$) over 6 weeks. GM2 decreased by approximately 40% ($p \leq 1.04e^{-12}$). The results are compiled from five different experiments. Although both HEXA linked only to the transferrin binding motif alone or fused only with G-CSF were each able to variably lower brain GM2, mTr-G-CSF-HEXA was more consistently effective and was, therefore, selected as the lead compound in this study (data not shown). As seen in Figure 7A, the effect on GM2 was dose related.

mTr-G-CSF-HEXA has a positive effect on the strength of the forelimbs in treated TS mice

Since the phenotypic properties of the TS $\text{HEXA}^{-/-}$ mice are variable and only become gradually discernible in the second year of life, we actively examined the physical strength in placebo-treated and mTr-G-CSF-HEXA-treated TS mice. Forelimb strength of each of the mice was measured before and after 6 weeks of intervention. The difference is expressed as percent change, where a negative change signifies a decrease and a positive change indicates a gain in strength. In Figure 8 (left), vehicle/placebo-treated male mice (control group) showed an overall 17% decrease in forelimb grip strength within the 6-week duration of the experiment, whereas the mTr-G-CSF-HEXA-treated mice (250 μg , IV; twice a week) experienced, on average, a

17% gain in strength ($p < 0.029$). Forelimb grip strength either remained stable ($\pm 2\%$) or increased (by $>2\%$) in two of nine and seven of nine in the placebo- and chimeric protein-treated mice, respectively ($p < 0.05$; chi-square test). Within 6 weeks, there was a 34% difference between the forelimb strength of the treated vs. placebo-treated mice. Figure 8, right, depicts the effects on forelimb grip strength of control group or increasing doses of mTr-G-CSF-HEXA (62.5 μg , 125 μg or 250 μg , each twice a week, over 6 weeks) in female mice. Again, placebo-treated mice lost strength within 6 weeks. However, even in low dose-treated female mice, no loss of strength was discernible. Using the high-dose (250 μg $\times 2/\text{week}$), forelimb grip strength significantly increased ($p < 0.00119$), resulting, again, in a 34% difference compared with placebo-treated mice observed within 6 weeks. Also, forelimb grip strength either remained stable ($\pm 2\%$) or increased (by $>2\%$) in 2 of 8 and 8 of 10 in the placebo- and chimeric protein-treated mice, respectively ($p < 0.02$; chi-square test).

DISCUSSION

In this report, we used the long-established Trojan horse approach for protein delivery across the BBB, which is modified, for the first time, to include a dual BBB entry mechanism rather than a single Trojan horse carrier. This novel method, applied to a model of adult TS in mice, is conceptually summarized in Figure 2C.

The transport across the BBB of very large protein, such as beta-hexosaminidase A, composed of two subunits encoded by two separate gene, HEXA and HEXB, each eventually transcribed into approximately 500 amino acid sequences, seems to be formidable. It is, therefore, notable that the engineered Tr-G-CSF-HEXA administered via peripheral delivery, was able to dose dependently and substantially decrease brain GM2. It should be further considered that brain GM2 accumulated during more than a full year of life was decreased by approximately 40% within just 6 weeks of treatment, in association with a gain of forelimb muscle strength. As such, this report suggests a treatment-related sizable effect on the course of the disease. This

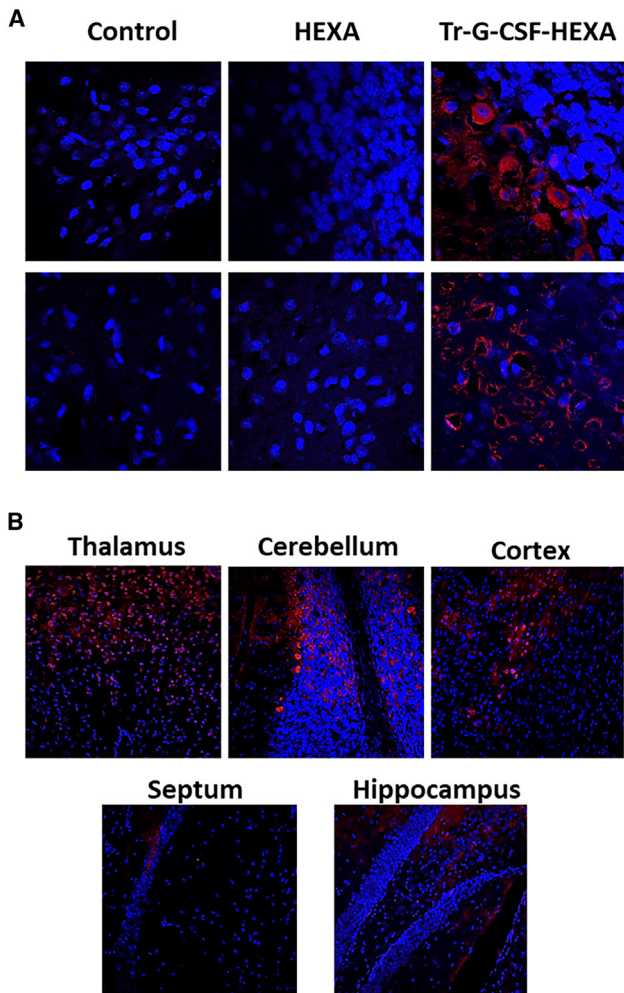


Figure 5. Brain sections of mice following peripheral injection (IV) of vehicle, or mHEXA (650 μ g, which is equimolar to the injected mTr-G-CSF-HEXA) or mTr-G-CSF-HEXA (1,000 μ g)

Using high magnitude confocal microscopy with immuno-fluorescent detection ($\times 100$), mTr-G-CSF-HEXA, but not HEXA, was clearly seen in the brain (Figure 5A) collected 3 h after its injection. The bright red staining represents the injected protein probed with anti-4-His tag. Nuclei are visualized in blue (stained with DAPI). The preferential cytoplasmic localization of the injected protein can be seen in cells where mTr-G-CSF-HEXA, in red, is present around the DAPI-stained nuclei. Specifically, mTr-G-CSF-HEXA was present in the cortex, thalamus, cerebellum, and hippocampus, and to a lesser degree at the septum (Figure 5B). As shown, mTr-G-CSF-HEXA is present in brain sections collected 3 h, 3 days, or 7 days following a single IV injection of Tr-G-CSF-Hexa-6 His (1,000 μ g). The protein was detected with anti-tetra-his immunostaining (red) and the blue color represents the brain nuclei stained with DAPI.

treatment effect is, then, distinct from the prevention of disease by neonatal or early-onset treatment modalities, in a disease characterized by late onset.

On this background, earlier studies examined the possibility to treat TS using small molecules that easily cross the BBB and could poten-

tially lower brain GM2. Miglustat, an inhibitor of glycosphingolipid biosynthesis, was effective in decreasing brain GM2 in a TS mouse model,²⁰ but failed to favorably affect the disease course in human subjects with LOTS.²¹ Venglustat, a second-generation substrate reducing agent has improved CNS penetration and is currently in clinical trials for LOTS and late onset Sandhoff's disease (NCT04221451). Pyrimethamine, shown to enhance HexA activity *in vitro*, apparently acting as a protein chaperone,²² did not achieve clinical benefits in LOTS patients in two clinical trials, using either an escalating dose or cyclic administration.^{23,24}

In recent years, gene delivery using viral vectors such as several adeno-associated virus (AAV) serotype elicited favorable effects in the treatment of TS models in small animals, initially through direct injection of the virus into the CNS, thereby bypassing the BBB, but subsequently even via peripheral administration.^{25–30} In an early report, Guidotti et al.²⁵ found that, to overcome the deficient alpha subunit of the heterodimeric protein HexA in TS, only overexpression of both subunits through peripheral co-administration of adenoviral vectors encoding HEXA and HEXB was able to sufficiently increase serum HexA (42% of wild-type levels). Direct injection to the brain of several viral vectors encoding either HEXA or HEXB or both seemed to yield impressive improvements in brain GM2 and extended the lifespan of mice with the rapidly progressing and lethal Sandhoff's disease if injected early enough in the post-natal weeks (26–30). Observations that AAV9-based vectors carrying a number of genes were shown to penetrate the BBB via peripheral administration and correct abnormal metabolism and storage in several disease models, including TS, potentially obviated the need for direct injections to the brain.^{31–35} Several related examples in humans that are based on the principles outlined above include the current clinical use of nusinersen, an oligonucleotide sequence injected intrathecally to treat infantile or late-onset spinal atrophy^{36,37}; onasemnogene abeparvovec, a single dose of IV AAV9 carrying the complementary DNA encoding the missing survival motor neuron 1³⁸; and, last, risdiplam, an orally administered, small molecule that modifies SMN2 pre-mRNA splicing and increases levels of functional SMN protein,³⁹ thus entirely bypassing the need to overcome the BBB.

Several reports indicated that modified AAV vectors carrying modified HEXA or HEXB subunits were able to favorably affect GM2 gangliosidosis. In two related reports, Tropak and colleagues⁴⁰ and Karumuthil-Melethil et al.⁴¹ designed and applied a modified alpha subunit incorporating specific beta-subunit sequences required to form a stable, HexB-like homodimer, and those sequences needed for the homodimer to interact with the GM2AP-GM2 complex, which they termed HEXM. This homodimer has HexA-like activity and could be expressed from a single gene packageable within a self-complementary AAV vector. To avoid potential liver toxicity⁴² or carcinogenesis,⁴³ which may occur with high-dose AAV9 vectors, they elected to pack HEXM into an advanced form of AAV9 vector, AAV9.47, which affords substantially diminished targeting to the liver but maintains high brain penetration with IV administration. When administered IV to neonatal TS mice, HEXM transgene achieved long-term GM2 reduction. In adult TS mice, it was capable of degrading GM2 in a

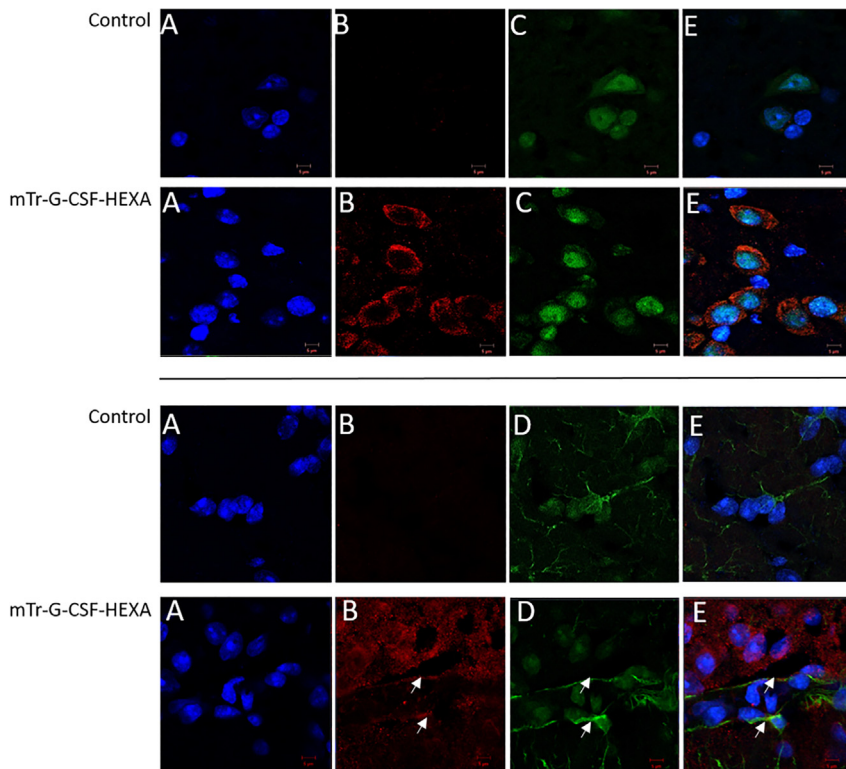


Figure 6. Detection of mTr-G-CSF-HEXA in TS mouse brain neurons and glial cells 3 h after an IV injection of 1 mg of mTr-G-CSF-HEXA-6HIS or vehicle (control)

mTr-G-CSF-HEXA-6HIS is visualized in red in neurons (top) and some glial cells (bottom) and can be seen in neuronal nuclei, using anti-6HIS antibody (red, B). Neuronal cells are identified by an anti-NeuN (green, C) and the nuclei were stained with DAPI (blue, A). And at lower anti-GFAP antibody (in green [D], identifies glial cells) and superposition of (A, B and C/D) is presented in (E). The white arrows point to the area where Tr-G-CSF-HEXA accumulated in glial cells. The brain sections were visualized using confocal microscopy ($\times 100$).

localized manner when injected intracranially. Thus, at the present time, this novel approach is effective as systemic therapy early on, but requires local intracranial delivery in the adult TS mouse. Whether this relates to the immaturity of the BBB in early life vs. fuller maturity in adult mice⁴⁴ or changes in mice size with maturation is unclear. A recent report in an ongoing study of two infants with infantile TS using an AAV (an equimolar mix of AAVrh8-HEXA and AAVrh8-HEXB) gene therapy delivered intrathecally around the cisterna magna and the thoracolumbar junction showed some disease deceleration.⁴⁵

Finally, ERT is widely applied in several non-CNS lysosomal disorders.⁴⁶ Selective replacement of only the mutated subunit in TS, HEXA was discarded 20 years ago, after a report that even large amounts of the soluble α subunit to cultured TS fibroblasts failed to reach the lysosomes in a sufficient quantity to hydrolyze cell GM2.¹⁴ However, Kitakaze et al.⁴⁷ generated a modified HexB, that, following direct intracerebroventricular injection to the CNS, was able to lower brain GM2 10-week-old Sandhoff mice, preceding the rapid neurological deterioration typical for this disease model.

In all, then, at the present time, the systemic treatment of adult TS, rather than prevention in neonates with TS, remains an experimentally and clinically unmet challenge. Therefore, the findings in our report that HEXA alone as well as hTr-G-CSF-HEXA decreases GM2 in human TS glial cells and that HEXA lowers GM2 in PBMC cultures harvested from LOTS patients would support the notion that HEXA per se, presumably associating with endogenous unmutated HEXB in TS, confers the ability

to lower GM2. Potential additional or alternative pathways were not pursued in the present report. Rather, we present a chimeric protein that carries HEXA as the therapeutic element, transported through the BBB by two independent Trojan horses poised in succession. This is the first description of a dual entry approach to carry a large enzyme/enzyme subunit across the BBB. This is also the first description of G-CSF as a *trans*-BBB carrier. Both HEXA and G-CSF retain their respective activities, which are relevant to TS: HEXA to lower GM2 and G-CSF, known to cross the intact BBB^{16,17} and, potentially, promote cell survival (which entails receptor binding). The idea that the transferrin receptor, which is broadly expressed on cells comprising the BBB can serve as an anchor to enzyme and protein delivery has been proposed by Partridge more than two decades ago.⁴⁸ Antibodies to the transferrin receptors and other ligands have been also tried [reviewed by Boado⁴⁹ and Partridge⁵⁰], of which we selected a short sequence that binds to the Tr receptor. Either Tr or G-CSF fused alone to HEXA showed GM2-lowering effect in adult TS mice, but the impact was more consistent when the chimeric protein combined both motifs. An inherent and potentially important advantage of the dual entry element approach is that it may be less susceptible to physiological or random inter-individual variability in receptor expression for either transferrin or G-CSF receptor; for example, the first is known to vary inversely to iron balance⁵¹ and the latter shows random widespread variability of expression in the human brain⁵² and may be down-regulated by inflammation and some cytokines such as tumor necrosis factor- α ⁵³ or interleukin-1 β ,⁵⁴ which could be overexpressed in late TS.⁵⁵ Our study has several limitations. Unlike humans, mice can use some compensating action by neuraminidase { sialidase } that can recycle hexosaminidase B cleavage products in the lysosome,⁵⁶ thereby limiting disease severity and delaying symptoms, reminiscent of the late and gradual course of human LOTS. However, Tr-G-CSF-HEXA is not related to sialidase and still can not only lower brain GM2, but elicit improvement in forelimb muscle strength.

We did not segregate the independent kinetics and contribution of the G-CSF element and the Tr element to the *trans*-BBB trafficking of Tr-G-CSF-HEXA. Both elements showed entry effects in

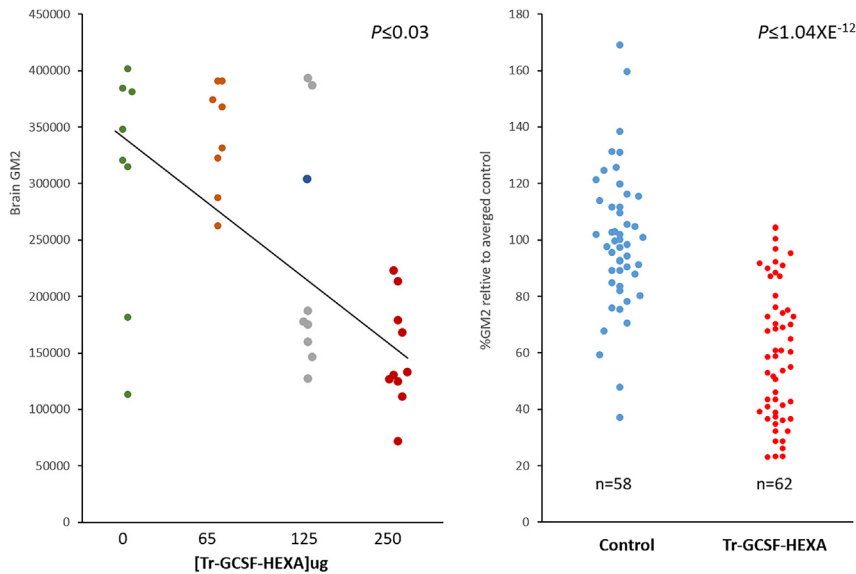


Figure 7. Chronic intravenously administered Tr-G-CSF-HEXA lowers brain GM2 concentrations

(A) mTr-G-CSF-HEXA treatment reduces brain GM2 of TS mice in a dose-dependent manner. Shown are levels of brain GM2 (expressed as arbitrary units) following the IV injection of 65, 125 and 250 μg ($*p \leq 0.003$.) mTr-G-CSF-HEXA or vehicle administered twice a week to the tail vein of 14- to 15-month-old female TS mice for 6 weeks.

(B) Chronic treatment with 250 μg Tr-G-CSF-HEXA markedly reduced brain GM2 in TS mice ($**p \leq 1.04E-12$). Shown are levels of brain GM2 (measured by LC-MS/MS and expressed as percent mean GM2 in the control TS mice) following of 250 μg Tr-G-CSF-HEXA or vehicle (200 μL) injections, administered twice a week via the tail vein of male and female TS mice for 6 weeks.

independent studies with Tr-HEXA or G-CSF-HEXA. However, this was less consistent in terms of GM2 reduction than the bimodal molecule, which suggest that the relative contribution of each of the entry elements may be variable *in vivo*. We did not quantify the percentage of the injected protein entering the brain or its penetration, but did observe that the protein enters other tissues as well, such as the heart and kidneys, which are not protected by entry barriers such as the BBB. The finding that there Tr-G-CSF-HEXA was practically undetectable in the liver suggests that the relative between-tissue distribution may vary with time. Finally, because transferrin as well as G-CSF receptors are present in non-CNS tissues, the possibility of unwanted effects in some non-brain target organs cannot be ruled out. The exclusion of any potential side effects by G-CSF may require further testing. It is noteworthy, however, that blood count was not affected by repeated administration of Tr-G-CSF-HEXA during the 6 weeks of the *in vivo* experiments. Last, we did not address the potential ability of G-CSF per se to enhance skeletal muscle regeneration⁵⁷ or neuronal stem cell differentiation in the brain.⁵⁸

In conclusion, the current study offers three major advancements regarding the treatment of LOTS and, possibly, beyond. First, we show that replacement therapy based on the replacement with the native, unmodified alpha subunit of HEXA alone can lower brain GM2 in human TS cells, including PMBCs from LOTS patients and in a mouse model of LOTS. Second, we show that this treatment is effective, in terms of brain GM2 and increase in muscle strength even in the adult mouse at a phase in which forelimb strength is already declining. Last, we present a *trans*-BBB delivery system of peripherally injected proteins that can enter the brain using a dual entry mechanism: utilization of the well-described transferrin receptor *trans*-BBB transport coupled with the herein first described G-CSF-dependent delivery. Since G-CSF per se may have neuroprotective effects^{16,17} and remains active in the fusion protein described in this report, this may confer potential additional benefits in neurodegenerative diseases.

MATERIALS AND METHODS

Production of HEXA and HEXB

The α -subunit and β -subunit of human or mouse β -hexosaminidase A (accession numbers hHEXA NP 000511; mHEXA NP 034551; hHEXB NP 000512; mHEXB NP 034552; all accession numbers are from GeneBank) were produced using a mammalian expression system in HEK293T or Expi293 cells. The gene was cloned into the pTT5 expression vector (Addgene); the resulting construct contained the codon for the signal peptide of mouse kappa IgG sequence at the N-terminus followed and by a 6-His tag at the C-terminus. HEK293T cells were grown in DMEM supplemented with 10% fetal bovine serum (FBS) (Invitrogen) at 37°C, 7.5% CO₂, which were humidified and agitated at 120 RPM. The cells were transfected with pTT5-HEXA plasmid, the medium was collected after 4–5 days post-transfection, and centrifuged at 2,000 $\times g$ for 30 min. The cleared supernatant was supplemented with 1.5% mannitol (Merck) and 0.01% Tween80 (Merck). The His-tagged proteins were concentrated on Ni-NTA (HisTrap) column, eluted with imidazole gradient (10–500 mM) and found purify to approximately 99% by SDS-PAGE.

Expression of fusion proteins

DNA sequences of the fusion proteins included a codon for the signal peptide of mouse kappa IgG sequence at the N-terminus and six-histidine at the C-terminus were cloned into pTT5 mammalian expression vector and consecutively expressed under the regulation of CMV promoter. The fusion proteins were produced recombinantly by the cellular expression system Expi293F (Invitrogen) in which the fusion protein was secreted into the extracellular medium. The cell suspension was humidified and agitated at 120 RPM at 37°C, 7.5% CO₂. The medium was collected 4–5 days post-transfection and centrifuged at 2,000 $\times g$ for 30 min. The cleared supernatant was supplemented with 1.5% mannitol (Merck) and 0.01% Tween80 (Merck), and the His-tagged proteins was purified from medium in one step on an Ni-NTA column using an imidazole gradient (5–500 mM). The eluted protein peak (300–400 mM imidazole) was concentrated, buffer exchanged (PBS, 3% mannitol 0.01% T-80) and then

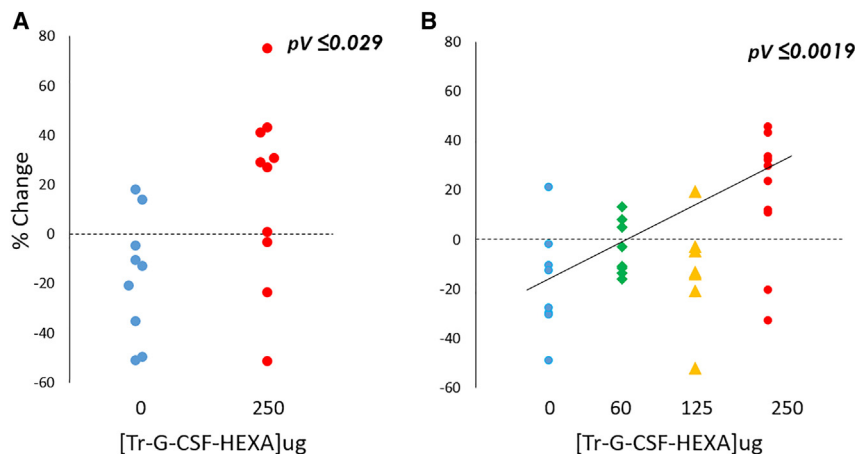


Figure 8. Chronic treatment with Tr-G-CSF-HEXA increases forelimb grip strength in 14- to 15-month-old TS male (left, $p \le 0.029$) and female (right, $p \le 0.0019$) mice (HEXA^{-/-}) (Left) Percent change in forelimb grip-strength before and after 6 weeks of treatment with 250 μ g Tr-G-CSF-HEXA or vehicle (200 μ L) injected to the tail vein of female TS mice twice a week**

(Right) Dose response of forelimb grip-strength changes before and after 7 weeks treatment with 65, 125, and 250 μ g Tr-G-CSF-HEXA or vehicle (200 μ L) injected to the tail vein of female TS mice twice a week. Each point represents an individual change in strength between the pre- and post-treatment state for each tested animal.

maintained at -80°C . The purity (approximately 99%) was detected by SDS-PAGE and probed by western blot using anti-tetra His (Qiagen) antibody or anti-mouse G-CSF antibody (R&D Systems).

The fusion proteins were concentrated and purified by binding to Ni-column via the C-terminus six-histidine tail and eluted from the Ni-column using an imidazole gradient (5–500 mM). The eluted protein picks were collected, concentrated, dialyzed in a reconstitution buffer, which contained PBS, 3% mannitol, and 0.01% Tween 80, and then was maintained at -80°C . Alternatively, the eluted protein peaks were collected and dialyzed in 50 mM ammonium acetate buffer pH 4.5 to remove the imidazole buffer, and the proteins freeze-dried and kept until use at -80°C .

The final amino acid sequences of the peptides and proteins constituting the different domains of the fusion proteins are detailed as follows: (1) Transferrin receptor binding peptide: HAIYPRHGS; (17); (2) mouse G-CSF: VPLVTVSALPPSLPLPRSFLKLSLEQVRKIQASGSV LLEQLCATYKLCHEPELVLLGHSLGIPKASLSCSSQALQQTQCL SQLHSGLCLYQGLLQALSISPALAPTLDLLQLDVANFATTIWQQ MENLGVAPTVPQTSAMPAFTSAFQRRAGGVLAISYLQGFLETA RLALHHLA; (3) human G-CSF: ATPLGPASSLPQSFLKCLEQVRK IQGDGAALQEKLKCATYKLCHEPELVLLGHSLGIPWAPLSSCPSQA LQLAGCLSQLHSGLFYQGLLQALEGISPELGPTLDTLQLDVADF ATTIWQQMEELGMAPALQPTQGAMPAFASAFQRRAGGVLVA SHLQSFLEVSRYRVLRLHAQP; (4) a modified GS flexible linker: GSGSDRVYIHPFHLSGSGSGSGSGSGSGSGSGSGSGSGSG; (5) mHEXA protein: LWPWPQYIQTYYHRRYTYLPNNFQFRYHVSSA AQAGCVVLDEAFRRYRNLFLGSGSWPRPFSNKKQTLGKNILV VSVVTAECNEFPNLESVENYTLTINDDQCLLASETVWGALRGL ETFSQLVWKSAAEGTFFINKTKIKDFPRFPHRGVLLDTSRHYLPLS SILDTLDVMAYNKFNVFHWHLVDDSSFPYESTFPPELTKRGSFN PVTHIYTAQDVKEVIEYARLRGIRVLAEFDTPGHTLSWGPAGP LLTPCYSGSHLSGTFGPVNPNSLNTYDFMSTLFLFLEISSVFPDFYLH LGGDEVDFTCWKSNPNIAFMKKKGFDFKQLESFYIQTLLDI VSDYDKGYVVWQEVFDNKVVRPDTIIQVWREMPVEYMLE MQDITRAGFRALLSAPWYLNVRVYKGPDWKDMYKVEPLAFHG TPEQKALVIGGEACMWGEYVDSTNLVPRWLPRAGAVAERLW

SSNLTNIDFAFKRLSHFRCELVRRGIQAQPISVGYCEQEFEQT; and (6) hHEXA protein: LWPWPQNFTSDQRYVLYPNNFQFQ YDVSSAAQPGCSVLDEAFQRYRDLFLGSGSWPRPYLTGKRHTL EKNVLVVSVVTPGCNQLPTLESVENYTLTINDDQCLLSETVW GALRGLTFSQLVWKSAAEGTFFINKTEIEDFPRFPHRGLLDTSR HYLPLSILDTLDVMAYNKLNVFHWHLVDDPSFPYESTFPPELM RKGSPNVTHIYTAQDVKEVIEYARLRGIRVLAEFDTPGHTLSW GPGIPGLLTPCYSGSEPSGTFGPVNPNSLNTYEFMSTFFLEVSSVF PDFYLHLLGGDEVDFTCWKSNPEIQDFMRKKGFEDFKQLESFY IQTLLDIVSSYGKGYVVWQEVFDNKVQIOPDTIIQVWREDIPVN YMKELELVTKAGFRALLSAPWYLNRSYGPDWKDFYIVEPLAFE GTPEQKALVIGGEACMWGEYVDSTNLVPRWLPRAGAVAER LWSNKLSTDLTFAYERLSHFRCELLRRGVQAQPLNVGFCEQE FEQT.

Various peptide linkers were used to link the two-domain carrier, mouse Tr-G-CSF and mouse HEXA. We selected the linker that afforded the best expression and also retained enzymatic activity. Screening was carried out according to the ability of the various generated fusion proteins to degrade GM2 in cultured human TS glia cells (originally derived from a TS embryo, kindly provided by Prof. Ruth Navon). Thus, the following *in vivo* studies were performed using mouse fusion proteins comprising Tr-G-CSF-peptide, the selected linker and HEXA, in succession.

Immunoprecipitation experiments

hTS glial cells incubated with or 40 μ g/mL (0.45 μ M) hHEXA-6His or vehicle for 16 h. Cells were then washed three times with ice-cold PBS and lysed with RIPA buffer (R0275 Merck) supplemented with a protease inhibitor (P2714 Merck) by agitation (100 RPM) for 30 min at 4°C . The cell’s lysate was collected and centrifuged at $11,000\times g$ for 10 min. Clear supernatants were incubated with anti-His in and Protein A and G Sepharose magnetic beads (17152104011150, Cytiva) for 16 h at 4°C , then washed three times and boiled with SDS sample buffer. The presence of HEXB was then detected by western blot chemiluminescence with anti hHEXB (Abcam, 140649) followed by anti-rabbit-Fc horseradish peroxidase (HRP)-linked antibody.

Analytical size exclusion chromatography for mTr-G-CSF-HEXA in different buffer formulas

mTr-G-CSF-HEXA was purified using Ni column and the purified protein peak was divided and buffer exchanged against three different buffer formulations: (1) 10 mM Na₂HPO₄, 1.8 mM KH₂PO₄, 137 mM NaCl, 2.7 KCl, pH7.4, 3% mannitol, 0.01% T80; (2) 50 mM Na Na₂HPO₄, 50 mM arginine, 3% mannitol, 0.05% T80, pH 8, and (3) 100 mM citrate, 22 mM arginine, 5% trehalose, 0.05% T80, pH 5. The oligomeric state of the protein in each formula solution was analyzed by an analytical Superdex 200 10/30 GL column pre-equilibrated with the same formula solution. We injected 100 µL of protein (1 mg/mL) into the column and elution was carried out with appropriate formula solution, respectively. The elution volume of the protein in each formula is presented in the [Figure S2A](#) and the protein sizes were extrapolated from paralleled analytical size exclusion chromatography of protein standards (Blue Dextran-2,000 kDa; apoferritin 443 kDa; amylose 200 kDa; alcohol dehydrogenase 150 kDa) performed individually for each protein formula.

Cells and cell culture

Human TS neuroglia cells were initially prepared from the cerebellum of an 18-week-gestation aborted TS fetus with infantile TS disease.⁵⁹ We verified the involved mutation as homozygous HEXA c.1421+1G>C, a variant located in a canonical splice site, which results in exon skipping and disruption of the reading frame. TS cells were grown in complete DMEM supplemented with 10% FBS, penicillin (100 U/mL), streptomycin (0.1 mg/mL), amphotericin (0.25 µg/mL), and L-glutamine (1%). The human normal glial cell line A-172 (American Type Culture Collection) was kindly provided by Prof M. Gavish, Technion, Haifa, Israel). Cells were grown in RPMI 1640 medium supplemented with FBS (10%), penicillin (100 U/mL) streptomycin (0.1 mg/mL), amphotericin (0.25 µg/mL), and L-glutamine (1%). Human TS glial cells were incubated with 100 µg/mL mTr-G-CSF-HEXA or mG-CSF-HEXA for 16 h.

The use of PBMCs of LOTS disease patients for this study was approved by the institutional review board (IRB). Four subjects diagnosed with LOTS carrying the α G269S/1278insTACT and three healthy controls, were recruited for the study. Patient characteristics are presented in [Tables S1](#) and [S2](#). PBMCs were used in primary culture, cells were isolated from whole blood using Lymphoprep standard methods (AXIS-SHIELD PoC AS). Heparinized whole blood samples collected no longer than 2 h before further processing were diluted 1:1 with PBS and were layered over the Lymphoprep density gradient and centrifuged for 45 min at 500×g at 25°C. The lymphocyte containing band was collected and washed twice with PBS and then collected by 15 min centrifugation at 400×g. Cells were plated with RPMI 1640 medium supplemented with fetal calf serum (10%), penicillin-streptomycin- amphotericin (1%) and L-glutamine (1%) and were treated with the recombinant human α -subunit of β hexosaminidase A at different concentrations ranging between 20 and 80 µg/mL or, as a control, TWEEN 80, 0.03% in PBS (vehicle) for 24–72 h in 12- or 96-well plates (each well seeded with 250,000 cells) at 37°C in a humidified incubator flushed continuously with a

5% CO₂ in air. In some experiments, M6P (Sigma) was added to the conditioned medium (at a final concentration of 10 mM). Cells were then analyzed for HexA activity or GM2 content. Following the various incubation protocols, treated and untreated cultured TS cells, glia cells or PBMC, plates were washed with PBS four times and harvested by scraping, washing twice with PBS followed by centrifugation at 1,500×g for 10 min during which the cell pellet was obtained.

Cell lysates were prepared by re-suspension of the cell pellet in 50 mM citrate buffer (pH 4.5). The resultant preparation underwent freezing in liquid nitrogen and thawing at 37°C for eight cycles. Following centrifugation at 12,000×g for 20 min at 4°C, the supernatant was collected and stored at a temperature of –20°C for HEXA enzymatic assay.

HexA activity

HexA enzymatic activity of purified fusion proteins or in cells was determined by using an artificial substrate for the enzyme activity: MUGS, which can be cleaved by HEXA, HexA but not HEXB.⁶⁰ For cell studies, human TS glial or peripheral blood mononuclear cells (PBMCs) from LOTS patients were incubated with various concentrations of HEXA, mTr-G-CSF-HEXA or mG-CSF-HEXA for 18–24 h. Following four washes, intracellular HexA activity was measured by HexA enzymatic activity assay, in which MUGS is used as a fluorescent substrate, and activity was expressed in arbitrary units. To measure HexA activity, cell or tissue extracted protein samples were incubated separately with the MUGS (1.6 mM; Melford Laboratories) in 50 mM citrate buffer (pH 4.5; 37°C) for 15 min. The fluorescence of the liberated 4-methylumbelliferone was measured by a fluorometer (excitation 335 nm, emission 442 nm). In some experiments, the apparent K_m was calculated by the Michaelis-Menten equation.

To test whether or not the recombinant mHEXA associates with mHEXB, we pre-coated a MaxiSorp with 10 µg/well of recombinant mHEXB or BSA, which was then blocked with 10% BSA in PBS. Plates were subsequently incubated with HEXA alone or HEXA fused to carrier proteins (mTr-G-CSF-HEXA or G-CSF-HEXA; 20 µg each) dissolved in citrate buffer (pH 4.5). Bands corresponding with captured HEXA-containing peptides are shown in [Figure S2B](#). In a second set of experiments, mHEXB was likewise first immobilized on a MaxiSorp-immune plate. Nonspecific binding of mTr-G-CSF-HEXA was blocked by 5% BSA. Trapped HEXB was then incubated with mTr-G-CSF-HEXA, followed by repeated washes to remove unbound mTr-G-CSF-HEXA. Enzymatic activity was then measured as a function of added mTr-G-CSF-HEXA concentrations. Bound mTr-G-CSF-HEXA was calculated from a standard curve of the HEXA-enzymatic-activity of mTr-G-CSF-HEXA concentrations. The experimental dissociation constant (K_d) was 166 nmol/L ([Figure S2C](#)).

Animals

The use of mice was approved by the Tel Aviv-Sourasky IRB for experimental use of animals. TS mice were kindly provided by

Professor Roy Gravel, at the University of Calgary, Canada. They were originally generated by disruption of the HEXA gene by homologous recombination. The construct used for targeted disruption of the HEXA gene was interrupted in exon 11 by a neomycin-resistance gene cassette.^{56,61} Homozygous mutant mice exhibit GM2 ganglioside accumulation in the brain as found in the human disease, but do not develop visible neurological deficiency until the second year of life. This is due to a delayed and slow accumulation of GM2 ganglioside in the mouse brain. However, HexA activity is practically absent in all tissues. Mice were housed in a room with a 12-h light/12-h dark cycle. Mutant TS mice were identified by PCR analysis of tail DNA with specific primers. Primers for detection of mutated HEXA sequences were: primer1: 5'-GGCCAGATACAATCATACAG and primer2: 5'-CTGTCCACATACTCTCCCCACAT. Phosphoglycerate kinase-1 promoter PGKneo vector sequences were recognized by primer 3: 5'-CACCAAAGAAGGGAGCCGGT.

G-CSF activity

The G-CSF activity of Tr-G-CSF-HEXA was measured by its ability to promote the survival of M-NFS-60 cells. M-NFS-60 cells were maintained in RPMI-1640 medium, with 10% FBS, 0.05 mM 2-mercaptoethanol, and 62 ng/mL human recombinant M-CSF. Cells were maintained for 3 days with increasing concentrations of mTr-G-CSF-HEXA or hG-CSF (Neupogen; Amgen) in the absence of M-CSF. Cell concentration was quantified by XTT cell proliferation assay Kit (Bet-Haemek) and the half-maximal effective concentration was calculated using the Hill equation.

Quantitative immunohistochemistry for GM2

TS neuroglial cells or PBMCs from patients with LOTS were plated on 96 well plates (8 × 10⁴ cells/mL) in quadruplicate for each hHEXA dilution and incubated overnight at 37°C. Following this initial incubation, hHEXA protein was added in serial dilutions ranging between 0 and 80 µg/mL. Cells were incubated for 48 h at 37°C and then washed three times with PBS at room temperature. Cells were fixed using 4% PFA/PBS for 5 min and then permeabilized with 0.03% Triton X100 for 5 min, washed with PBS, and blocked with 5% BSA/PBS overnight at 4°C. Cells were then immunostained with rabbit anti-GM2 antibody (Calbiochem; dilution 1:200) for 2 h. Following initial washing with PBS/0.03% Tween 80, cells were treated with anti-rabbit HRP-conjugated antibody (Jackson Immuno Research Laboratories, Inc). After additional washing, a color reaction was developed using TMB/E reagent (Millipore) and the reaction was stopped with 1 N HCl solution. The absorbance was measured with a microliter plate ELISA reader at 450 nm. This method was modified from Tsuji et al.⁶²

Immunofluorescence labeling for GM2

Intracellular GM2 ganglioside in treated and untreated TS cells was visualized by immunostaining. TS neuroglial cells were grown on glass discs in 12-well plates and incubated with different concentrations of added hHEXA or PBS/0.03% Tween 80, as control, for 24 h. The cells were then washed with PBS/0.01% Tween 20 to remove non-incorporated hHEXA protein, blocked with BSA 5% (Sigma-

Aldrich) and then stained with Rabbit anti-Ganglioside asialo GM2 Polyclonal Antibody (Calbiochem) as the primary antibody (dilution 1:800). The cells were then immunostained with goat anti-rabbit FITC- (Invitrogen). Phalloidin-TRITC (Sigma-Aldrich) diluted 1:800 was added to visualize cell membranes. Slides were mounted with Vestashield mounting medium containing DAPI (Vector Laboratories Ltd).

Immunohistochemical detection of the fusion proteins in the brain

The *in vivo* penetration of HEXA or the fusion proteins through the BBB into the brain was tested in wild-type mice which received a single IV injection of vehicle, HEXA or Tr-G-CSF-HEXA and were sacrificed with CO₂ after the injections at different time periods as indicated in Figures 5 and S5. To remove the entire blood volume containing the injected proteins from the brain, PBS solution was infused into the left ventricle (total of 30 mL, at least 6-fold of the mouse own blood volume) and blood was drained through the right atrium until the effluent was entirely clear of blood and the liver become pink, followed by perfusion with ice-cold 4% paraformaldehyde (PFA) in PBS (15 mL). Brain was then collected on ice and incubated at 4°C as follow: 4% PFA in PBS for 24 h, 15% sucrose in PBS for 24 h, and kept in 30% sucrose at least 2 days until brain slicing. Slices from each brain were incubated in citrate buffer pH 6 at 95°C for 30 min, stained with rabbit anti-histidine monoclonal antibody (Cayman Chemical), which detected with secondary antibody—donkey anti rabbit IgG H&L—Alexa Fluor555 (Abcam) and DAPI. In additional studies, 3-month-old TS mice were injected with 1 mg of mTr-G-CSF-HEXA-6His or vehicle (control). Three hours later, the mice were scarified and the brains were removed. We immune-stained 8 µM of brain sections. At the top of Figure 6, anti-6HIS (red, B) was used to detect mTr-GCSF-HEXA, anti-NeuN a nuclear marker for nerve cells (green, C) signaled neurons and nuclei were stained with DAPI (blue, A). In the lower panel of Figure 6, glial cells were visualized with anti-GFAP marker for glial cells (green, D), and the presence of mTr-GCSF-HEXA (red, B) was detected with anti-6HIS. The brain sections were visualized using confocal microscopy (×100) and superposition of A, B, and C/D is presented in E. The white arrows point to the area where Tr-G-CSF-HEXA accumulated in glial cells.

Extraction of brain GM2

Animals were sacrificed by CO₂ and perfused through the left ventricle with 30 mL of PBS solution. Blood was drained through the right atrium until the effluent was entirely clear of blood as detailed in the previous section. The brain was then immediately collected, placed in PBS (1:4, w/v) and homogenized on ice with a homogenizer-mixer (Heidolph, Instruments). The homogenate was then sonicated for 20 s with 20% output. Each of the elution procedures presented below included mixing for 30 s with a vortex. Initially, 70 µL of brain homogenate was extracted by adding 170 µL of chloroform/methanol (1/2 v/v), vortexed and then centrifuged for 5 min at 1,200×g. The upper phase was collected and the lower phase containing the pellet was re-extracted with 170 µL of chloroform/methanol (2/1 v/v and then vortexed and centrifuged at 1,200×g for 5 min.

Both supernatants were pooled and extracted again with 170 μ L of chloroform and 100 μ L water. The mixture was centrifuged at $4,000\times g$ for 5 min, and the upper phase was collected. The lower phase was re-extracted with 360 μ L of methanol/water (2/1 v/v) for 30 s followed by centrifugation at $10,000\times g$ for 5 min. The upper phases were pooled and vacuum-dried in speed-vac at 40°C , for approximately 2 h). The dried pellet was dissolved in 250 μ L of water and the resultant GM2-enriched fraction was eluted twice with 250 μ L of water-saturated butanol and then centrifuged at $9,700\times g$ for 5 min. Both butanol phases were combined and vacuum-dried at $40^{\circ}\text{--}45^{\circ}\text{C}$ for about approximately 2 h. For GM2 measurement, the dried pellet was dissolved in 200 μ L of methanol and triplicate aliquots (50 μ L) of each sample were measured by LC-MS/MS.

Measuring brain GM2 by LC-MS/MS analysis

All analytical equipment was from Agilent Technologies and consisted of a 6545 QTOF mass spectrometer with an electrospray ionization interface (ESI) coupled to a 1,260 ultra-high-performance liquid chromatography (UHPLC), a G4204A quaternary pump, G4226A ALS auto-sampler, and G1316C thermostatted column compartment. UHPLC was carried out on a ZORBAX RRHD Eclipse Plus C18, 95 \AA , 2.1×50 mm, 1.8- μ m column with 70% mobile phase A (30% tetrahydrofuran/20% methanol/50% 5 mM NH_4COOH in water) with gradient elution to 100% mobile B (70% tetrahydrofuran/20% methanol/10% 5 mM NH_4COOH in water) in 3 min and then another 3 min at 100% mobile phase B at a flow rate of 0.5 mL/min.⁶³ Five microliters of each sample and standard were injected into the LC-MS/MS instrument in triplicate, and an average peak area of three analyses was calculated. Methanol solution was injected as a blank within a sequence of samples to confirm that there was no cumulative carryover. We injected 1 mg/mL GM2 methanolic solution as a standard. The ESI was operated in negative mode. Detection of GM2 was monitored by the ion transitions 1382.808 m/z $[\text{M-H}]^- \rightarrow 290.088$ m/z. Mass spectral parameters were optimized for GM2 by the fragmentor voltage of the ion source to 220, where source temperature was set to 300°C , drying gas 8 L/min, nebulizer 40 psi, sheath gas temperature 400°C , and sheath gas flow 12L/min 400°C . Ion spray voltage was 4.5 kV and collision and energy for product ion mode (MS/MS) was 80 V.⁶²

Forelimb strength

Forelimb strength was monitored automatically with a force sensor connected electronically to Grip Strength Meter (UGO). When mice are pulled back by the tail, they instinctively grab the grid of the grip strength meter, to try to stop this involuntary backward movement, until the pulling force overcomes their grip strength. Each measurement is the mean of seven different pulling challenges separated from each other by 5 s. The difference between the force measured before and at the end of treatment was then calculated for each mouse separately as percent change relative to baseline. Negative changes imply loss of strength over the 6 weeks of the experiment, whereas positive changes imply gain of strength.

Statistical analysis

Statistical analysis was performed using SPSS 17 software. Differences between the mean values obtained from the experimental and the control groups were evaluated by Student's t-test, parametric ANOVA, or non-parametric tests (Mann-Whitney, Wilcoxon). A *p* value of less than 0.05 was considered significant.

DATA AND CODE AVAILABILITY

All raw data supporting the findings are available from the corresponding Authors upon reasonable request.

SUPPLEMENTAL INFORMATION

Supplemental information can be found online at <https://doi.org/10.1016/j.omtm.2024.101300>.

ACKNOWLEDGMENTS

The authors wish to acknowledge the generous funding support of The Chief Scientist's Office of the Israeli Ministry of Health; The Israeli Innovation Authority, Israel; The Sagol Foundation, Israel; and The LOTS Research Donation Fund at TLVMC, Israel. The authors wish to express their gratitude to Prof. Roy Gravel for providing the Late Onset Tay Sachs mice for the experiments in this work.

AUTHOR CONTRIBUTIONS

E.O., Y.A., R.S.S., N.U., T.U., S.A., G.W., F.K., M.W., Y.S., and N.S., performed the experiments. E.O., Y.A., R.S.S., N.U., and N.Stern., analyzed the data. E.O., Y.A., R.S.S., N.U., O.B., A.V., A.F.V., L.S., R.N., M.W., and N.Stern., discussed the data. E.O., Y.A., and N.Stern., conceived, designed, and supervised the research. E.O., Y.A., and N. Stern., wrote the manuscript. All authors read and approved the manuscript.

DECLARATION OF INTERESTS

N.Stern, E.O., O.B., and Y.A. are inventors in patent WO 2022/180628. N.Stern, E.O., and R.N. are inventors in patent US20100183577A1.

REFERENCES

1. Gravel, R., Kaback, M., Proia, R., Sandhoff, K., Suzuki, K., and Suzuki, K. (2001). The GM2 gangliosidosis. In *The Metabolic and Molecular Basis of Inherited Disease*, 8th Ed, Scriver, A.L. Beaudet, D. Valle, and W.S. Sly, eds. (McGraw-Hill), pp. 3827–3876.
2. Mahuran, D.J. (1999). Biochemical consequences of mutations causing the GM2 gangliosidosis. *Biochim. Biophys. Acta* 1455, 105–138.
3. Neufeld, E.F. (1991). Lysosomal storage diseases. *Annu. Rev. Biochem.* 60, 257–280.
4. Lemieux, M.J., Mark, B.L., Cherney, M.M., Withers, S.G., Mahuran, D.J., and James, M.N.G. (2006). Crystallographic structure of human beta-hexosaminidase A: interpretation of Tay-Sachs mutations and loss of GM2 ganglioside hydrolysis. *Mol. Biol.* 359, 913–929.
5. Proia, R.L., d'Azzo, A., and Neufeld, E.F. (1984). Association of alpha- and beta-subunits during the biosynthesis of beta-hexosaminidase in cultured human fibroblasts. *Biol. Chem.* 259, 3350–3354.
6. Ghosh, P., Dahms, N.M., and Kornfeld, S. (2003). Mannose 6-phosphate receptors: new twists in the tale. *Nat. Rev. Mol. Cell Biol.* 4, 202–212.
7. Little, L.E., Lau, M.M., Quon, D.V., Fowler, A.V., and Neufeld, E.F. (1988). Proteolytic processing of the alpha-chain of the lysosomal enzyme, beta-hexosaminidase, in normal human fibroblasts. *J. Biol. Chem.* 263, 4288–4292.

8. Navon, R., Padeh, B., and Adam, A. (1973). Apparent deficiency of hexosaminidase A in healthy members of a family with Tay-Sachs disease. *Am. J. Hum. Genet.* 25, 287–293.
9. Neudorfer, O., Pastores, G.M., Zeng, B.J., Gianutsos, J., Zaroff, C.M., and Kolodny, E.H. (2005). Late-onset Tay-Sachs disease: phenotypic characterization and genotypic correlations in 21 affected patients. *Genet. Med.* 7, 119–123.
10. Riboldi, G.M., and Lau, H. (2022). Diagnostic Tips from a Video Series and Literature Review of Patients with Late-Onset Tay-Sachs Disease. *Tremor Other Hyperkinet Mov. (N Y)* 2, 34.
11. Desnick, R.J., and Schuchman, E.H. (2002). Enzyme replacement and enhancement therapies: lessons from lysosomal disorders. *Nat. Rev. Genet.* 3, 954–966.
12. Partdrige, W.M. (2005). Molecular biology of the blood-brain barrier. *Mol. Biotechnol.* 30, 57–70.
13. Guidotti, J., Akli, S., Castelnuovo-Ptakhine, L., Kahn, A., and Poenaru, L. (1998). Retrovirus-mediated enzymatic correction of Tay-Sachs defect in transduced and non-transduced cells. *Hum. Mol. Genet.* 7, 831–838.
14. Martino, S., Emiliani, C., Tancini, B., Severini, G.M., Chigorno, V., Bordignon, C., Sonnino, S., and Orlacchio, A. (2002). Absence of metabolic cross-correction in Tay-Sachs cells: implications for gene therapy. *J. Biol. Chem.* 277, 20177–20184.
15. Zhao, L.R., Navalitloha, Y., Singhal, S., Mehta, J., Kessler, J.A., Piao, C.S., Guo, W.P., and Groothuis, D.R. (2007). Hematopoietic growth factors pass through the blood-brain barrier in intact rats. *Exp. Neurol.* 204, 569–573.
16. Wallner, S., Peters, S., Pitzer, C., Resch, H., Bogdahn, U., and Schneider, A. (2015). The granulocyte-colony stimulating factor has a dual role in neuronal and vascular plasticity. *Front. Cell Dev. Biol.* 3, 48.
17. Schneider, A., Krüger, C., Steigleder, T., Weber, D., Pitzer, C., Laage, R., Aronowski, J., Maurer, M.H., Gassler, N., Mier, W., et al. (2005). The hematopoietic factor G-CSF is a neuronal ligand that counteracts programmed cell death and drives neurogenesis. *J. Clin. Invest.* 115, 2083–2098.
18. Calipari, E.S., Godino, A., Peck, E.G., Salery, M., Mervosh, N.L., Landry, J.A., Russo, S.J., Hurd, Y.L., Nestler, E.J., and Kiraly, D.D. (2018). Granulocyte-colony stimulating factor controls neural and behavioral plasticity in response to cocaine. *Nat. Commun.* 9, 9.
19. Youn, P., Chen, Y., and Furgeson, D.Y. (2014). A myristoylated cell-penetrating peptide bearing a transferrin receptor-targeting sequence for neuro-targeted siRNA delivery. *Mol. Pharm.* 11, 486–495.
20. Platt, F.M., Neises, G.R., Reinkensmeier, G., Townsend, M.J., Perry, V.H., Proia, R.L., Winchester, B., Dwek, R.A., and Butters, T.D. (1997). Prevention of lysosomal storage in Tay-Sachs mice treated with N-butyldeoxyjirimycin. *Science* 276, 428–431.
21. Shapiro, B.E., Pastores, G.M., Gianutsos, J., Luzy, C., and Kolodny, E.H. (2009). Miglustat in late-onset Tay-Sachs disease: a 12-month, randomized, controlled clinical study with 24 months of extended treatment. *Genet. Med.* 11, 425–433.
22. Maegawa, G.H., Tropak, M., Buttner, J., Stockley, T., Kok, F., Clarke, J.T., and Mahuran, D.J. (2007). Pyrimethamine as a potential pharmacological chaperone for late-onset forms of GM2 gangliosidosis. *J. Biol. Chem.* 282, 9150–9161.
23. Osher, E., Fattal-Valevski, A., Sagie, L., Urshanski, N., Amir-Levi, Y., Katzburg, S., Peleg, L., Lerman-Sagie, T., Zimran, A., Elstein, D., et al. (2011). Pyrimethamine increases β -hexosaminidase A activity in patients with Late Onset Tay Sachs. *Mol. Genet. Metab.* 102, 356–363.
24. Osher, E., Fattal-Valevski, A., Sagie, L., Urshanski, N., Sagiv, N., Peleg, L., Lerman-Sagie, T., Zimran, A., Elstein, D., Navon, R., et al. (2015). Effect of cyclic, low dose pyrimethamine treatment in patients with Late Onset Tay Sachs: an open label, extended pilot study. *Orphanet J. Rare Dis.* 10, 45.
25. Guidotti, J.E., Mignon, A., Haase, G., Caillaud, C., McDonnell, N., Kahn, A., and Poenaru, L. (1999). Adenoviral gene therapy of the Tay-Sachs disease in hexosaminidase A-deficient knock-out mice. *Hum. Mol. Genet.* 8, 831–838.
26. Cachón-González, M.B., Wang, S.Z., Lynch, A., Ziegler, R., Cheng, S.H., and Cox, T.M. (2006). Effective gene therapy in an authentic model of Tay-Sachs-related diseases. *Proc. Natl. Acad. Sci. USA* 103, 10373–10378.
27. Sargeant, T.J., Wang, S., Bradley, J., Smith, N.J., Raha, A.A., McNair, R., Ziegler, R.J., Cheng, S.H., Cox, T.M., and Cachón-González, M.B. (2011). Adeno-associated virus-mediated expression of β -hexosaminidase prevents neuronal loss in the Sandhoff mouse brain. *Hum. Mol. Genet.* 20, 4371–4380.
28. Cachón-González, M.B., Wang, S.Z., McNair, R., Bradley, J., Lunn, D., Ziegler, R., Cheng, S.H., and Cox, T.M. (2012). Gene transfer corrects acute GM2 gangliosidosis—potential therapeutic contribution of perivascular enzyme flow. *Mol. Ther.* 20, 1489–1500.
29. Bradbury, A.M., Gray-Edwards, H.L., Shirley, J.L., McCurdy, V.J., Colaco, A.N., Randle, A.N., Christopherson, P.W., Bird, A.C., Johnson, A.K., Wilson, D.U., et al. (2015). Biomarkers for disease progression and AAV therapeutic efficacy in feline Sandhoff disease. *Exp. Neurol.* 263, 102–112.
30. Cachón-González, M.B., Wang, S.Z., Ziegler, R., Cheng, S.H., and Cox, T.M. (2014). Reversibility of neuropathology in Tay-Sachs-related diseases. *Hum. Mol. Genet.* 23, 730–748.
31. Weismann, C.M., Ferreira, J., Keeler, A.M., Su, Q., Qui, L., Shaffer, A.S., Xu, Z., Gao, G., and Sena-Estev, M. (2015). Systemic AAV9 gene transfer in adult GM1 gangliosidosis mice reduces lysosomal storage in CNS and extends lifespan. *Hum. Mol. Genet.* 24, 4353–4364.
32. Walia, J.S., Altaieb, N., Bello, A., LaFave, M.C., Varshney, G.K., Burgess, S.M., Chowdhury, B., Hurlbut, D., Hemming, R., Hemming, R., et al. (2015). Long-term correction of Sandhoff disease following intravenous delivery of rAAV9 to mouse neonates. *Mol. Ther.* 23, 414–422.
33. Gadalla, K.K., Bailey, M.E., Spike, R.C., Ross, P.D., Woodard, K.T., Kalburgi, S.N., Bachaboina, L., Deng, J.V., West, A.E., Samulski, R.J., et al. (2013). Improved survival and reduced phenotypic severity following AAV9/MECP2 gene transfer to neonatal and juvenile male Mecp2 knockout mice. *Mol. Ther.* 21, 18–30.
34. Fu, H., Dirosario, J., Killedar, S., Zaraspe, K., and McCarty, D.M. (2011). Correction of neurological disease of mucopolysaccharidosis IIIB in adult mice by rAAV9 trans-blood-brain barrier gene delivery. *Mol. Ther.* 19, 1025–1033.
35. Ruzo, A., Marco, S., Garcia, M., Villacampa, P., Ribera, A., Maggioni, A.L., Mingozzi, F., Haurigot, V., and Bosch, F. (2012). Correction of pathological accumulation of glycosaminoglycans in central nervous system and peripheral tissues of MPSIIIA mice through systemic AAV9 gene transfer. *Hum. Gene Ther.* 23, 1237–1246.
36. Finkel, R.S., Mercuri, E., Darras, B.T., Connolly, A.M., Kuntz, N.L., Kirschner, J., Chiriboga, C.A., Saito, K., Servais, L., Tizzano, E., et al. (2017). Nusinersen versus sham control in infantile-onset spinal muscular atrophy. *N. Engl. J. Med.* 377, 1723–1732.
37. Mercuri, E., Darras, B.T., Chiriboga, C.A., Day, J.W., Campbell, C., Connolly, A.M., Iannaccone, S.T., Kirschner, J., Kuntz, N.L., Saito, K., et al. (2018). Nusinersen versus sham control in later-onset spinal muscular atrophy. *N. Engl. J. Med.* 378, 625–635.
38. Mendell, J.R., Al-Zaidy, S., Shell, R., Arnold, W.D., Rodino-Klapac, L.R., Prior, T.W., Lowes, L., Alfano, L., Berry, K., Church, K., et al. (2017). Single-dose gene-replacement therapy for spinal muscular atrophy. *N. Engl. J. Med.* 377, 1713–1722.
39. Baranello, G., Darras, B.T., Day, J.W., Deconinck, N., Klein, A., Masson, R., Mercuri, E., Rose, K., El-Khairi, M., Gerber, M., et al. (2021). Risdiplam in type 1 spinal muscular atrophy. *N. Engl. J. Med.* 384, 915–923.
40. Tropak, M.B., Yonekawa, S., Karumuthil-Melethil, S., Thompson, P., Wakarchuk, W., Gray, S.J., Walia, J.S., Brian L Mark, J.W., and Mahuran, D. (2016). Construction of a hybrid β -hexosaminidase subunit capable of forming stable homodimers that hydrolyze GM2 ganglioside *in vivo*. *Mol. Ther. Methods Clin. Dev.* 3, 15057.
41. Karumuthil-Melethil, S., Kalburgi, S.N., Thompson, P., Tropak, M., Kaytor, M.D., Keimel, J.G., Mark, B.L., Mahuran, D., Walia, J.S., and Gray, S.J. (2016). Novel Vector Design and Hexosaminidase Variant Enabling Self-Complementary Adeno-Associated Virus for the Treatment of Tay-Sachs Disease. *Hum. Gene Ther.* 27, 509–521.
42. Hinderer, C., Katz, N., Buza, E.L., Dyer, C., Goode, T., Bell, P., Richman, L.K., and Wilson, J.M. (2018). Severe Toxicity in Nonhuman Primates and Piglets Following High-Dose Intravenous Administration of an Adeno-Associated Virus Vector Expressing Human SMN. *Hum. Gene Ther.* 29, 285–298.
43. Donsante, A., Miller, D.G., Li, Y., Vogler, C., Brunt, E.M., Russell, D.W., and Sands, M.S. (2007). AAV vector integration sites in mouse hepatocellular carcinoma. *Science* 317, 477.
44. Banks, W.A., Reed, M.J., Logsdon, A.F., Rhea, E.M., and Erickson, A. (2021). Healthy aging and the blood-brain barrier. *Nat. Aging* 1, 243–254.

45. Flotte, T.R., Cataltepe, O., Puri, A., Batista, A.R., Moser, R., McKenna-Yasek, D., Douthwright, C., Gernoux, G., Blackwood, M., Mueller, C., et al. (2022). AAV gene therapy for Tay-Sachs disease. *Nat. Med.* 28, 251–259.
46. Garbade, S.F., Zielonka, M., Mechler, K., Kölker, S., Hoffmann, G.F., Staufner, C., Mengel, E., and Ries, M. (2020). FDA orphan drug designations for lysosomal storage disorders - a cross-sectional analysis. *PLoS One* 15, e0230898.
47. Kitakaze, K., Mizutani, Y., Sugiyama, E., Tasaki, C., Tsuji, D., Maita, N., Hirokawa, T., Asanuma, D., Kamiya, M., Sato, K., et al. (2016). Protease-resistant modified human β -hexosaminidase B ameliorates symptoms in GM2 gangliosidosis model. *J. Clin. Invest.* 126, 1691–1703.
48. Shi, N., Boado, R.J., and Pardridge, W.M. (2001). Receptor-mediated gene targeting to tissues *in vivo* following intravenous administration of pegylated immunoliposomes. *Pharm. Res. (N. Y.)* 18, 1091–1095.
49. Boado, R.J. (2022). IgG Fusion Proteins for Brain Delivery of Biologics via Blood-Brain Barrier Receptor-Mediated Transport. *Pharmaceutics* 14, 1476.
50. Partridge, W.M. (2020). Blood-Brain Barrier and Delivery of Protein and Gene Therapeutics to Brain. *Front. Aging Neurosci.* 11, 373.
51. van Gelder, W., Huijskes-Heins, M.I., Cleton-Soeteman, M.I., van Dijk, J.P., and van Eijk, H.G. (1998). Iron uptake in blood-brain barrier endothelial cells cultured in iron-depleted and iron-enriched media. *J. Neurochem.* 71, 1134–1140.
52. Ridwan, S., Baue, r H., Frauenknecht, K., Hefti, K., von Pein, H., and Sommer, C.J. (2014). Distribution of the hematopoietic growth factor G-CSF and its receptor in the adult human brain with specific reference to Alzheimer's disease. *J. Anat.* 224, 377–391.
53. Elbaz, O., Budel, L.M., Hoogerbrugge, H., Touw, I.P., Delwel, R., Mahmoud, L.A., and Löwenberg, B. (1991). Tumor necrosis factor downregulates granulocyte-colony-stimulating factor receptor expression on human acute myeloid leukemia cells and granulocytes. *J. Clin. Invest.* 87, 838–841.
54. Shieh, J.H., Gordon, M., Jakubowski, A., Peterson, R.H., Gabrilove, J.L., and Moore, M.A. (1993). Interleukin-1 modulation of cytokine receptors on human neutrophils: *in vitro* and *in vivo* studies. *Blood* 81, 1745–1754.
55. Jeyakumar, M., Thomas, R., Elliot-Smith, E., Smith, D.A., van der Spoel, A.C., d'Azzo, A., Perry, V.H., Butters, T.D., Dwek, R.A., and Platt, F.M. (2003). Central nervous system inflammation is a hallmark of pathogenesis in mouse models of GM1 and GM2 gangliosidosis. *Brain* 126, 974–987.
56. Miklyeva, E.I., Dong, W., Bureau, A., Fattahie, R., Xu, Y., Su, M., Fick, G.H., Huang, J.Q., Igdoura, S., Hanai, N., and Gravel, R.A. (2004). Late onset Tay-Sachs disease in mice with targeted disruption of the Hexa gene: behavioral changes and pathology of the central nervous system. *Brain Res.* 1001, 37–50.
57. Wright, C.R., Ward, A.C., and Russell, A.P. (2017). Granulocyte Colony-Stimulating Factor and its potential application for skeletal muscle repair and regeneration. *Mediators Inflamm.* 2017, 7517350. <https://doi.org/10.1155/2017/7517350>.
58. Wu, C.C., Wang, I.F., Chiang, P.M., Wang, L.C., Shen, C.J., and Tsai, K.J. (2017). G-CSF-mobilized bone marrow mesenchymal stem cells replenish neural lineages in Alzheimer's disease mice via CXCR4/SDF-1 Chemotaxis. *Mol. Neurobiol.* 54, 6198–6212. <https://doi.org/10.1007/s12035-016-0122-x>.
59. Hoffman, I.M., Amsterdam, D., and Schneck, L. (1976). GM2* ganglioside in fetal Tay -Sachs disease brain cultures: a model system for the disease. *Brain Res.* 111, 109–117.
60. Hou, Y., Tse, R., and Mahuran, D.J. (1996). Direct determination of the substrate specificity of the alpha-active site in heterodimeric beta-hexosaminidase A. *Biochemistry* 35, 3963–3969.
61. Phaneuf, D., Wakamatsu, N., Huang, J.Q., Borowski, A., Peterson, A.C., Fortunato, S.R., Ritter, G., Igdoura, S.A., Morales, C.R., Benoit, G., et al. (1996). Dramatically different phenotypes in mouse models of human Tay-Sachs and Sandhoff diseases. *Hum. Mol. Genet.* 5, 1–14.
62. Tsuji, D., Higashine, Y., Matsuoka, K., Sakuraba, H., and Itoh, K. (2007). Therapeutic evaluation of GM2 gangliosidosis by ELISA using anti-GM2 ganglioside antibodies. *Clin. Chim. Acta* 378, 38–41.
63. Fuller, M., Duplock, S., Hein, L.K., Rigat, B.A., and Mahuran, D.J. (2014). Liquid chromatography/electrospray ionisation-tandem mass spectrometry quantification of GM2 gangliosides in human peripheral cells and plasma. *Anal. Biochem.* 458, 20–26.